



SCAPS-1D Simulation and Electrodeposition of Molybdenum Disulfide and Zinc Selenide for Optoelectronic Applications.

O. OLUBOSEDE^{*1}, A.A FAREMI², O.S ADIGBO³

Department of Physics, Federal University Oye – Ekiti. Nigeria

*Corresponding author E-mail address: olusayo.olubosede@fuoye.edu.ng

Abstract

Keywords:
SCAPS simulation, heterostructured device electrodeposition, photovoltaic device, solar cells

In this research work, ZnSe/MoS₂ based photovoltaic device were simulated using SCAPS simulation for the materials reproducibility in the laboratory. Having achieved the simulated materials, the materials were synthesized on a well-degreased Fluorine doped Tin Oxide substrates using simple, fast, and inexpensive 2-electrode configuration Electrodeposition (ED) technique. The optical properties and electrical conductivity of the film of ZnSe and MoS₂ were determined. The grown heterostructured ZnSe/MoS₂ on FTO substrate was numerically modeled by utilizing the experimentally obtained optical parameters in the SCAPS simulator for the extraction of the heterostructured device electrical parameters heterostructured based photovoltaic device. In the fabrication of photovoltaic cells, n-type ZnSe was first deposited on FTO using ED and heat-treated for 20 minutes in an oven furnace at temperature of 400^oC before immersing it into the solution containing the bath of MoS₂. The deposited structure of ZnSe formed a junction with MoS₂ using electrodeposition. The variation of substrate temperature which have an influence on the electrical parameters of the heterostructured based photovoltaic device was examined.

Accepted: 20 June, 2024

© Science Research Annals. All rights reserved.

INTRODUCTION

Semiconductors allow passage of electricity under certain conditions in response to a voltage. With this advantage over conductors and insulators, they have been used to engineer numerous types of electronic devices such as diodes, transistors, and optoelectronics (Jenkins, 2005). Photoconductivity involves the exposure semiconductor to photons with energy more than that of the semiconductor's energy band gap which is usually sunlight. Doping is basically the addition or introduction of impurities to the semiconductor material (Dimitrijević, 2011). Semiconductor materials have been reported as viable materials capable of addressing high cost of semiconductor-based devices with an improved efficiency (Zhang *et al.*, 2020). Among the various semiconductor materials, silicon and germanium have been the focus of research attention owing to the

promising potential in the field of science and industry (Yang *et al.*, 2022). However, the industrial application of silicon and germanium for the fabrication of photovoltaic device has a very low market penetration because of the expensive cost of silicon-based electronics devices (Al-Ezzi & Ansari, 2022). In the quest of circumventing the bottleneck placed by the utilization of silicon, research focus has been shifted to compound semiconductor materials because of their direct energy band gaps, cost effectiveness, high conversion efficiency, ease of production, etc (Faremi *et al.*, 2021a; Olusola *et al.*, 2020; Samuel Oluyamo & Akande Faremi, 2020). Most Solar Panels available commercially are at most 20% Power Conversion Efficiency which means approximately 80% of Power Conversion Efficiency is lost during the following process: (i) Radiative Recombination, (ii) Thermalization Loss, (iii) Non-

Absorption loss and (iv) Non-Radiative Recombination. According to NREL (National Renewable Energy Laboratory), the highest cell efficiency as at today is at 47.6% (Fig.5) (Green et al., 2023), This Laboratory monitors solar cells innovation around the world.

In this work, we take a look at electrodeposit heterostructured FTO/ZnSe/MoS₂ solar cell, determine of the conductivity type of the electrodeposited compound semiconductor; simulate heterostructured FTO/ZnSe/MoS₂ solar cell, compare the solar parameter achieved in the electrodeposition of the heterostructured solar cell and the simulation of the heterostructured solar cell and evaluate the effect of temperature on the JV characteristics, solar parameters and energy band diagram of the heterostructured solar cell.

MATERIALS AND METHODS

Methodology

Figure 1 depicts the device structure of the thin film

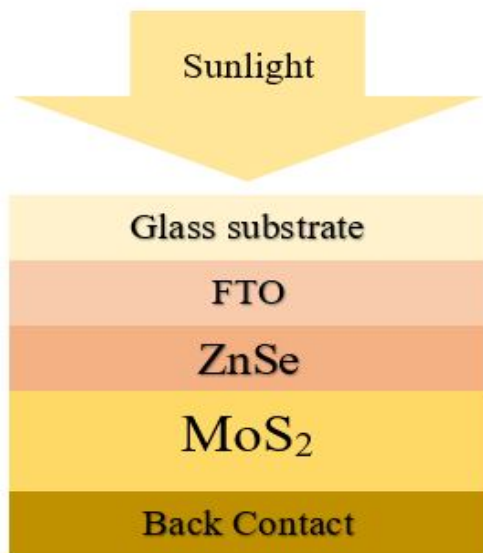


Figure 1 Device structure of the thin film

In this work, SCAPS-1D simulation software was extensively used for the numerical modelling of the materials. The SCAPS-1D simulation software solves semiconductor equations in one dimension, such as Continuity equation for electron and holes, Poisson's equation – relating the charge to the potential (Eq.1 and Eq. 2), and Current density for electrons and holes (Eq. 3 and Eq. 4) (Rassol et al., 2021; Sayed et al., 2011):

$$\frac{d^2\psi}{dx^2} = \frac{dE}{dx} = \frac{\rho}{\epsilon_0 \epsilon_T} \tag{1}$$

$$\frac{d^2\psi}{dx^2} = \frac{q}{\epsilon_0 \epsilon_T} [p(x) - n(x) + N_D - N_A + p_p - p_n] \tag{2}$$

Where ψ is electrostatic potential, q is elementary charge, ϵ_T is relative permittivity of the material, ϵ_0 is vacuum permittivity, p is hole concentration, n is electron concentration and are donor and acceptor charge concentrations respectively, and are holes and electrons distribution respectively. Eq.1 is the Poisson's equation of relation of electric field to the electrostatic potential with respect to the thickness. While Eq.3 is the Poisson's equation of the relation of the holes and electrons to the electrostatic potential.

Current density for electron and holes is being influenced mainly by drift equations which happens as a result of the electric field and diffusion equation which happens a result of the state of the material according to Eq.9 and Eq.10, respectively, Eq.8 can be derived at when the material is at equilibrium that is when the drift equation is equal to the negative of the diffusion equation this is from the Einstein relation:

$$D_n = \mu_n \frac{kT}{q}, D_p = \mu_p \frac{kT}{q} \tag{3}$$

(Einstein relation)

$$J_n = q \left(D_n \frac{dn}{dx} + \mu_n n \frac{d\psi}{dx} \right) \tag{4}$$

$$J_p = -q \left(D_p \frac{dp}{dx} + \mu_p p \frac{d\psi}{dx} \right) \tag{5}$$

Where ψ is potential difference, D_n and D_p are electron and hole diffusion coefficient, respectively. μ_n and μ_p are electron and hole mobility, J_n and J_p are electron and hole current density, respectively n and p are electron and hole carrier concentration (Sayed et al., 2011).

$$\frac{dJ_n}{dx} = \frac{dJ_p}{dx} = G - R$$

Where J_p and J_n are hole and electron current densities respectively, G and R are the net generation rate and net recombination rates respectively by external processes such as illumination by light (Sayed et al., 2011). Both heterostructured semiconductors were synthesised (Olubosede et.al, 2021).

$$T = \frac{ItM}{qnF} \tag{7}$$

The thin film's thickness as indicated in the above equation (Eq.7) is denoted as T, J is the current density of the electrodeposited compound semiconductor, t is the deposition time in seconds, ρ is the density of the electrodeposited compound

semiconductor n is the total number of electrons transferred per ion of the electrodeposited compound semiconductor, F is the Faraday's constant with a numerical value of $96,485 \text{Cmol}^{-1}$, and M is the molar weight of the electrodeposited compound semiconductor.

$$(\alpha h\nu) = A(h\nu - E_g)^n \tag{8}$$

α is the absorption coefficient of the electrodeposited compound semiconductor as denoted in (Eq.8), $h\nu$ is the incident photon energy, A is a constant usually equal to one, E_g is the energy band gap of the electrodeposited compound semiconductor, and n is the transition time between the valence band and conduction band of the electrodeposited compound semiconductor, which is 0.5 for direct and 1 for indirect transition.

$$\text{PEC Signal} = V_L - V_D \tag{9}$$

Where V_L is the voltage under illumination and V_D is the voltage under dark.

Results and Discussions

After the Implementation of the Electrodeposited technique for the for ZnSe thin films, MoS₂ thin films and a sandwiched ZnSe and MoS₂ we respectively have what can be seen in figure 2 to figure 4..

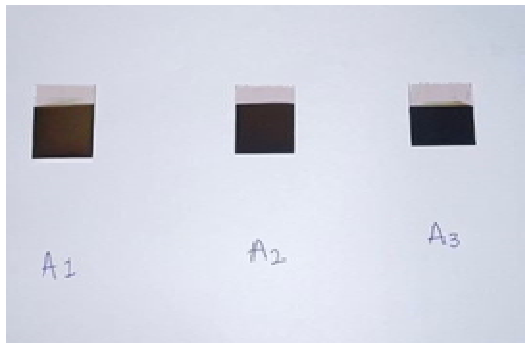


Figure 2: Electrodeposited MoS₂ at varied deposition time

Table 1 shows the Extracted properties of the electrodeposited materials at varied deposition time

Table 1: Extracted properties of the electrodeposited materials at varied deposition time

Extracted properties of the electrodeposited materials at varied deposition time						
Time of deposition (minute)	Thickness (nm)		Energy band gap (eV)		Electrical conductivity type	
	MoS ₂	ZnSe	MoS ₂	ZnSe	MoS ₂	ZnSe
5	62	135	2.17	2.46	P-type	N-type
10	144	172	2.02	2.16	P-type	N-type
15	198	205	1.87	2.03	P-type	N-type

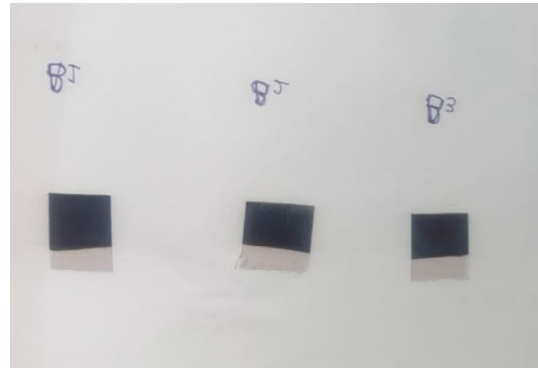


Figure 3: Electrodeposited ZnSe at varied deposition time



Figure 4: Electrodeposited heterostructured ZnSe/MoS₂

Comparing of the Results of Electrodeposited Heterostructured Glass/FTO/ZnSe/MoS₂ and the Simulation Results. We in have what is shown table 2.

Table 2: Comparison of the Experimental and Simulated Results

Solar Parameters	Experiment	Simulation
Open circuit Voltage	0.199	0.23526
short circuit current	1.4	1.0007
Fill factor	0.653	0.6754
Efficiency	1.82	1.7473
maximum voltage	0.182	0.17884
maximum current	1	0.97701

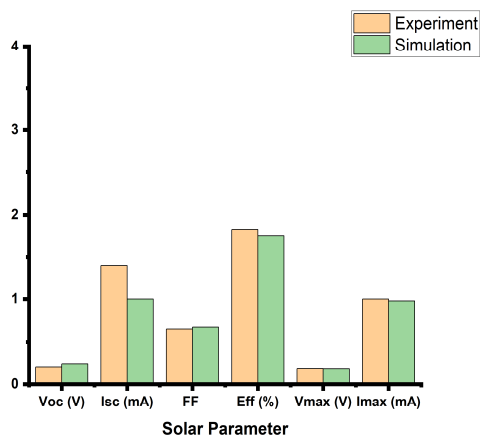


Figure 5: Comparison Bar chart of the Simulated and Experimental results

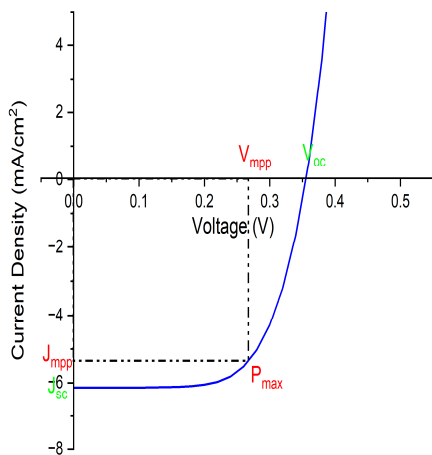


Figure 6: J-V Curve with the Solar Parameters.

Comparing of the Light and Dark Conditions J-V Curve Results

Figure 7 indicates the effect of illumination on the simulated results

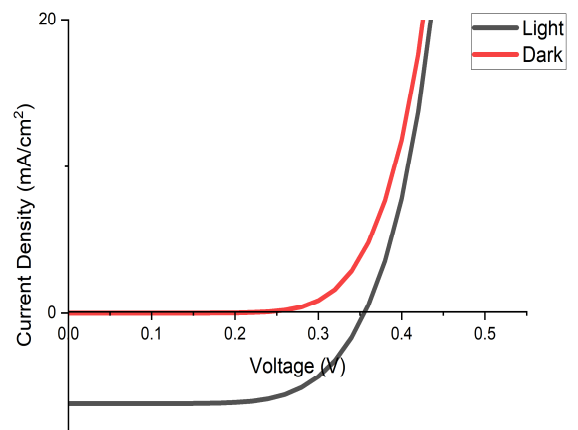


Figure 7 JV characteristics of both dark and light

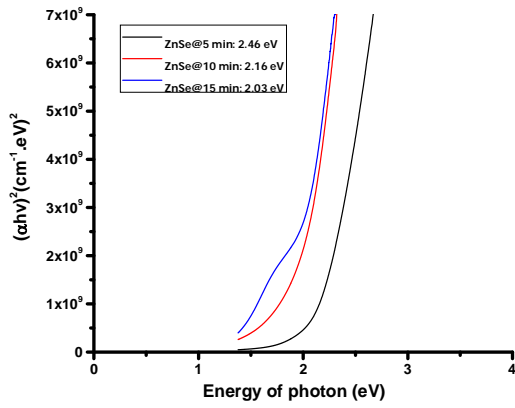


Figure 8: Variation of time of deposition with Energy band Gap of ZnSe

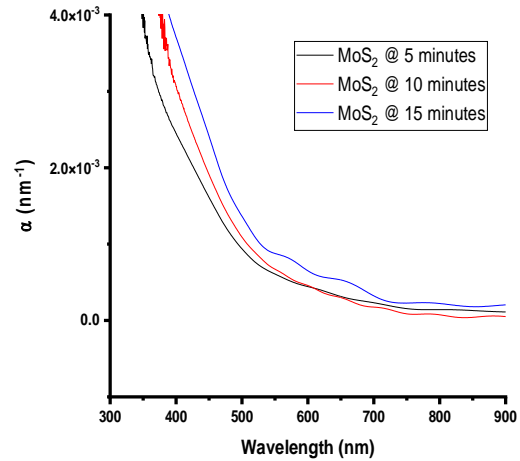


Figure 11: Variation of time of deposition with Absorption coefficient of MoS₂ as a function of wavelength.

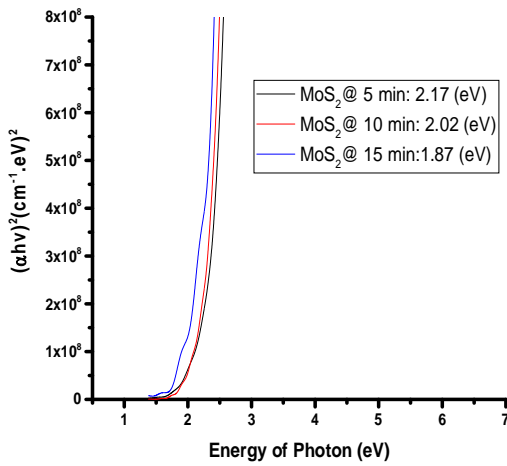


Figure 9: Variation of time of deposition with Energy band gap of MoS₂

The optical phenomena of the electrodeposited zinc selenide and that of molybdeum disulfide as a function of deposition time are shown in figure 10 and figure 11.

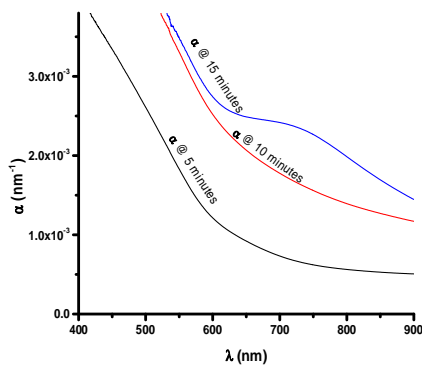


Figure 10: Variation of time of deposition with Absorption coefficient of ZnSe as a function of wavelength

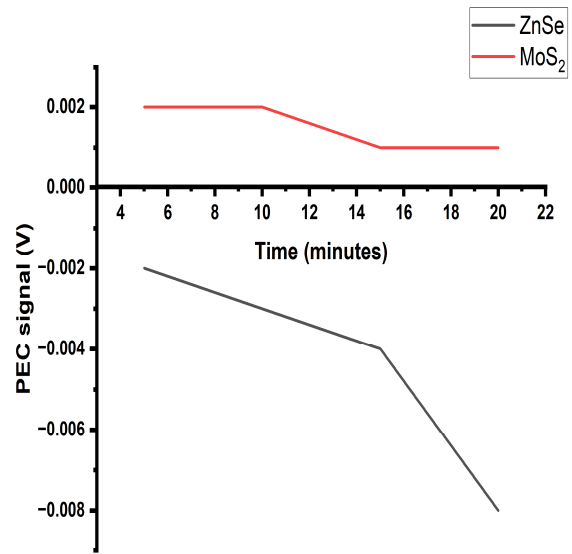


Figure 12: PEC signal for glass/FTO/ZnSe and glass/FTO/MoS₂ layers at varied time. PEC, photoelectrochemical cells

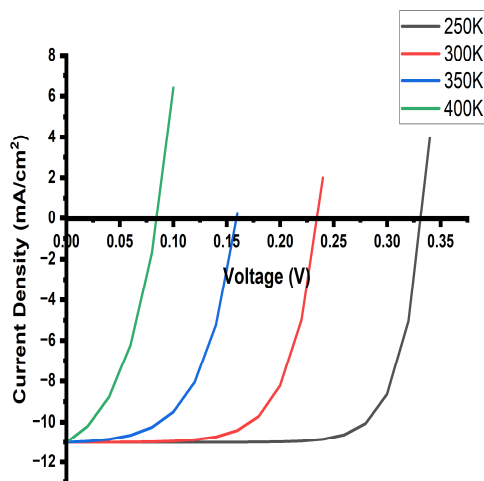


Figure 13: Effect of Temperature on the JV curve

Table 1.3: Effect of temperature on the Solar Parameters

Temperature	Efficiency (%)	V _{oc} (V)	J _{sc} (mA/cm ²)	FF (%)	V _{mpp} (V)	J _{mpp} (mA/cm ²)
400	0.39532	0.08497	10.99453	42.3177	0.05172	7.64406
350	0.98922	0.15939	10.99614	56.4423	0.11126	8.89149
300	1.74725	0.23526	10.99659	67.5394	0.17884	9.77008
250	2.82809	0.3326	10.99706	77.3213	0.27384	10.32754

It can be seen that the electrodeposited compound semiconductor energy band gaps decrease as the time increases (2.49-2.03eV), this shows that the thickness of the ZnSe material influences the energy band gap of ZnSe. From figure 4.5, which is for MoS₂, it was noticed that there are energy band gaps (2.17-1.87eV) are inversely proportional to the varied time of deposition, this also shows that the thickness of MoS₂ which is as a result of the deposition time influences band gaps of MoS₂.

The energy band gap values obtained from both ZnSe and MoS₂ as time increases. The noticed changes in the energy band gap of the electrodeposited compound semiconductors thin films are being caused by the quantum confinement effect which is being resulted from the dependence optical properties on the particle dimension, this phenomenon can be attributed to nanostructure engineering.

In this research, electrodeposited heterostructured Molybdenum disulfide and Zinc selenide thin film material was both numerically and experimentally modelled successfully, the obtained results for both simulation and experimental are in consonant.

Since solar cells would be used mainly for terrestrial use ignoring its use by NASA (National Aeronautics and Space Administration), solar cells would be integrated in to the environment which encompasses the weather and climate conditions, this is study has to take in to consideration by the engineers and scientist for future research of solar cells. Most semiconductor modelling is done at 300K since it is close to room temperature and a convenient number. The extracted electrical parameters at 300K show that the device can works efficiently at room temperature if scaled up to industrial level.

The solar cell performance is determined by its parameters such as short circuit current density, open circuit voltage, fill factor and efficiency. The open-circuit voltage and V_{mpp} are the major parameter which undergo steady decrease all through as a result of temperature. And also concerning the energy band gap, the reaction of FTO was noticed as it shrinks as a result of cold temperature and performs excellently for high temperature, this justifies claims of FTO having good thermal properties.

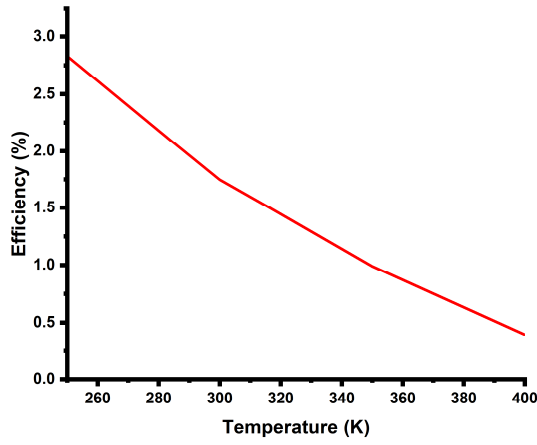


Figure 14: Effect of Temperature on the Efficiency

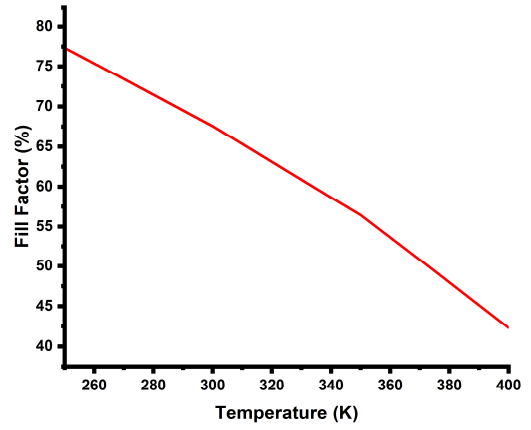


Figure 17 Effect of Temperature on the Fill Factor

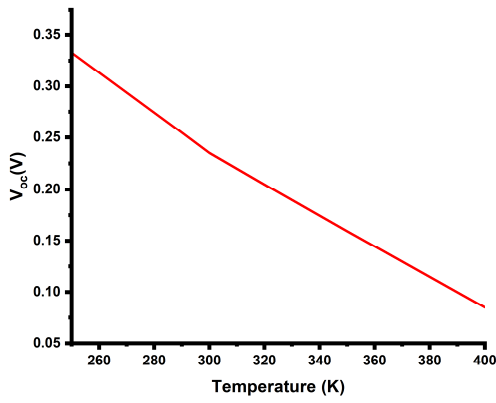


Figure 15: Effect of Temperature on the V_{oc}

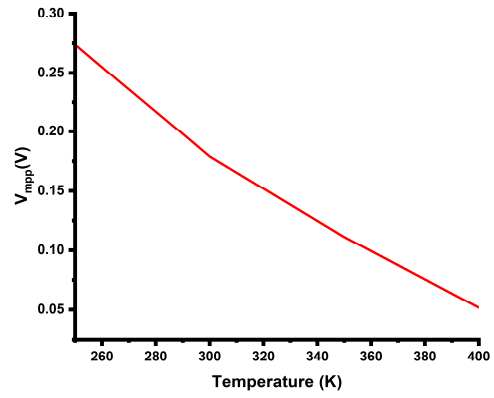


Figure 18: Effect of Temperature on the V_{mpp}

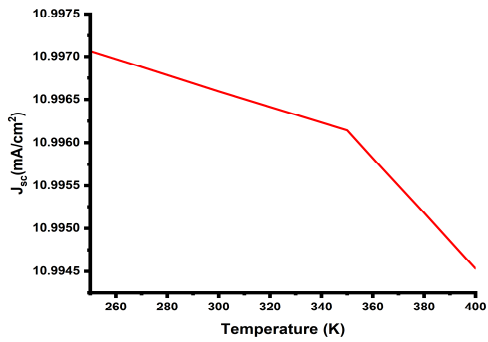


Figure 16: Effect of Temperature on the J_{sc}

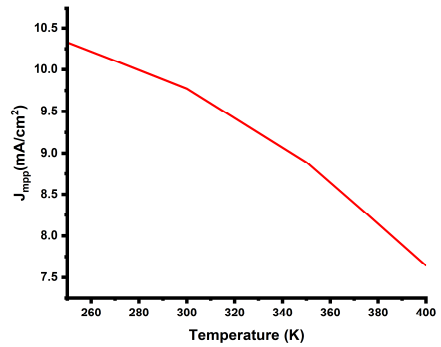


Figure 19: Effect of Temperature on the J_{mpp}

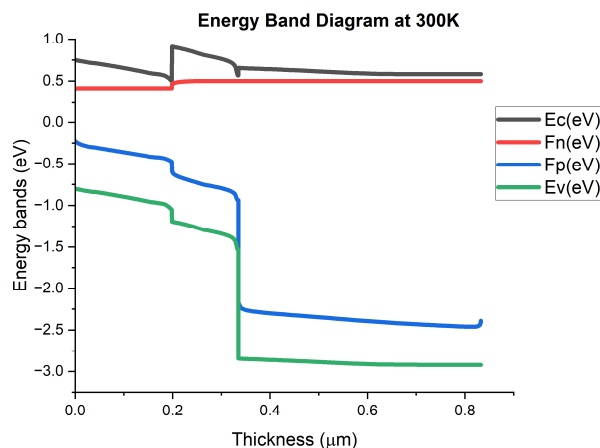


Figure 20: Energy Band Diagram of the electrodeposited compound semiconductor at room temperature. This shows the Effect of Temperature on the Energy Band

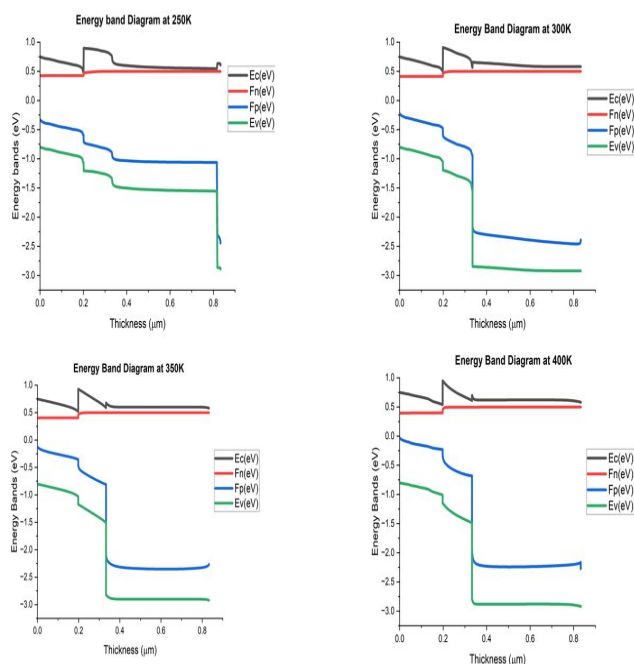


Figure 21: Effect of Temperature on the Energy Band Diagram

It can be seen that the electrodeposited compound semiconductor energy band gaps decrease as the time increases. the thickness of the ZnSe material influences the energy band gap of ZnSe. For MoS₂, it was noticed that there are energy band gaps are inversely proportional to the varied time of deposition, this also shows that the thickness of MoS₂ which is as a result of the deposition time influences band gaps of MoS₂. It infers that ZnSe material is a N-type material while MoS₂ is a P-type material.

REFERENCES

1. Akimoto, K., Ishizuka, S., Yanagita, M., Nawa, Y., Goutam, K. P. and Sakurai, T. (2006). "Thin film deposition of Cu₂O and

application for solar cells". *Solar Energy*, **80**: 715-722.

2. Asaduzzaman M, Bahar AN, Bhuiyan MMR, Habib MA. Impacts of temperature on the performance of CdTe based thin-film solar cell. *IOP Conf Ser Mater Sci Eng.* 2017; 225(1):012274; <https://doi.org/10.1088/1757-899X/225/1/012274>
3. Balitskii OA, Demchenko PY, Mijowska E, Cendrowski K. Synthesis and characterization of luminescent aluminium selenide nanocrystals. *Mater Res Bull.* 2013; 48(2):916-9; <https://doi.org/10.1016/j.materresbull.2012.11.059>
4. Beck G, Funk S. Correlation between optical appearance and orientation of aluminium. *Surf Coat Technol.* 2012; 206(8-9):2371-9; <https://doi.org/10.1016/j.surfcoat.2011.10.034> Lincot D. Electrodeposition of semiconductors. *Thin Solid Films.* 2005; 487(1-2):40-8; <https://doi.org/10.1016/j.tsf.2005.01.032>
5. Ceviz O I, Y. Odemir, M. Bedir and M. Ozaş, Effect of the substrate temperature on the characterization of spray-deposited ZnS: B films developed in science parks *Journal of Optoelectronics and Biomedical Materials* 5 (2013) 51-5
6. Echendu O.K, Okeoma K.B, Oriaku C.I, Dharmadasa I.M (2016). Electrochemical deposition of CdTe semiconductor thin films for solar cell application using two-electrode and three-electrode configurations: A comparative study. *Adv Mater Sci Eng.* 2016;10-14; <https://doi.org/10.1155/2016/3581725>
7. Ikhioya I. L. A. Chinecherem, S.N. Ezema, M. Maaza, F. Ezema, A study on the effects of varying concentrations on the properties of ytterbium-doped cobalt selenide thin films, *Opt. Mater.* 101 (2020) 109731, <https://doi.org/10.1016/j.optmat.2020.109731>.
8. Ikhioya L., D. N. Okoli, A. J. Ekpunobi, Electrochemical deposition of tin doped zinc selenide (SnZnSe) (2020) *Thin film material. Asian Journal of Nanoscience and Materials*, 3(3) 189-202
9. Khan N. A, A. Saleem, A. R. Satti, et al. Post deposition annealing: a route to bandgap tailoring of ZnSe thin films. *J. Mater. Sci-Mater.* El 27 (2016) 9755-9760. <https://doi.10.1007/s10854-016-5039-7>
10. Manoharan C., G. Pavithra, M. Bououdina, S. Dhanapandian and P. Dhamodharan. Characterization and study of antibacterial activity of spray pyrolysed ZnO: Al thin films *Applied Nanoscience* 6 (2016) 815-25

11. Mittal V., N. P. Sessions, J. S. Wilkinson, et al. Optical quality ZnSe films and low loss waveguides on Si substrates for mid-infrared. *Opt. Mater. Express* 7 (2017) 712–725. 11.
<https://doi.org/10.1364/OME.7.000712>
12. Olusola O.I, Oluyamo S.S, Ajayi O.A (2020). Materials science in semiconductor processing opto-electronic properties of electrodeposited ZnTe using zinc anode as counter electrode. *Mater Sci Semicond Process.*:105494;
<https://doi.org/10.1016/j.mssp.2020.105494>
13. Pandey, J 2015 Solar cell harvesting: Green renewable technology of future introduction. *Int. J. Adv. Res. Eng. Appl. Sci.*, 4, 93–103.
14. Salim HI, Patel V, Abbas A, Walls JM, Dharmadasa IM. Electrodeposition of CdTe thin films using nitrate precursor for applications in solar cells. *J Mater Sci Mater Electron.* 2015;26(5):3119–28;
<https://doi.org/10.1007/s10854-015-2805-x>
15. Slonopas A, Alijabbari N, Saltonstall C, Globus T, Norris P (2017). Thin Film Performance Optimization through Chemical Vapor Deposition. *International Journal of Electronic Networks, Devices and Fields.* ISSN 0974-2182, Volume 9 Number 1, Pp 1-10
16. Xia M, C. Liu, Z. Zhao (2015). Formation and optical properties of ZnSe and ZnS nanocrystals in glasses. *J. Non-Cryst. Solids* 429 79–82.
<https://10.1016/j.jnoncrysol.2015.08.034>